

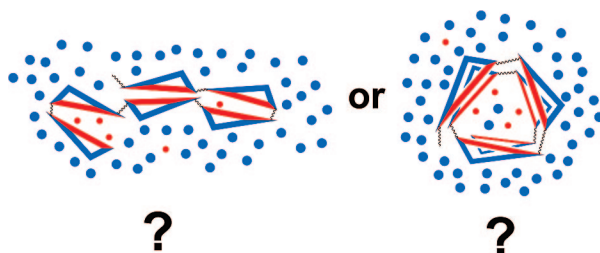
Conformation of Oligocholate Foldamers with 4-Aminobutyroyl Spacers

Yan Zhao[†]

Department of Chemistry, Iowa State University, Ames, Iowa 50011-3111

zhaoy@iastate.edu

Received October 2, 2008



Extended oligocholates with 4-aminobutyroyl groups in between the cholate units were labeled with a naphthyl and a dansyl at the chain ends. Fluorescence resonance energy transfer (FRET) from the naphthyl to the dansyl was observed in 2:1 hexane/ethyl acetate (EA) containing a few percent of methanol. An increase of methanol in the solvent caused unfolding of the extended oligocholates, diminishing the energy-transfer efficiency. The 4-aminobutyroyl spacers strongly influenced the conformation of the oligocholates. Whereas the parent oligocholates (with no spacing groups in between the cholates) require at least five cholate groups to fold cooperatively, the 4-aminobutyroyl-spaced oligocholates could do so in more competitive solvents with as few as three or four cholates.

Introduction

Foldamers, or linear oligomers mimicking biopolymers in their conformational behavior, have generated intense interest among scientists in multiple disciplines in recent years.^{1–3} Many have come to the realization that, if biofoldamers such as proteins, nucleic acids, and polysaccharides are able to perform sophisticated biological functions, synthetic foldamers with

analogous conformational properties should carry out similar tasks in structural support, molecular recognition, sensing, transport, and catalysis.

Hydrophobic interactions, salt bridges, and disulfide linkages essential to protein conformation come mostly from the

[†] Phone: 515-294-5845. Fax: 515-294-0105.

(1) For some representative reviews, see: (a) Hecht, S.; Huc, I., Eds. *Foldamers: Structure, Properties, and Applications*; Wiley-VCH: Weinheim, Germany, 2007. (b) Gellman, S. H. *Acc. Chem. Res.* **1998**, *31*, 173–180. (c) Kirshenbaum, K.; Zuckermann, R. N.; Dill, K. A. *Curr. Opin. Struct. Biol.* **1999**, *9*, 530–535. (d) Stigers, K. D.; Soth, M. J.; Nowick, J. S. *Curr. Opin. Chem. Biol.* **1999**, *3*, 714–723. (e) Hill, D. J.; Mio, M. J.; Prince, R. B.; Hughes, T. S.; Moore, J. S. *Chem. Rev.* **2001**, *101*, 3893–4012. (f) Cubberley, M. S.; Iverson, B. L. *Curr. Opin. Chem. Biol.* **2001**, *5*, 650–653. (g) Sanford, A. R.; Gong, B. *Curr. Org. Chem.* **2003**, *7*, 1649–1659. (h) Martinek, T. A.; Fulop, F. *Eur. J. Biochem.* **2003**, *270*, 3657–3666. (i) Huc, I. *Eur. J. Org. Chem.* **2004**, 17–29. (j) Licini, G.; Prins, L. J.; Scrimin, P. *Eur. J. Org. Chem.* **2005**, 969–977. (k) Goodman, C. M.; Choi, S.; Shandler, S.; DeGrado, W. F. *Nat. Chem. Biol.* **2007**, *3*, 252–262.

(2) Foldamers stabilized by directional forces such as hydrogen bonds and metal–ligand complexation tend to adopt highly organized, discrete, folded conformations, whereas those stabilized by nondirectional forces such as solvophobic interactions tend to be highly dynamic and interconvert between many degenerate folded states. Both types of folding are found in natural proteins. For a recent review on solvophobic foldamers, see: Zhao, Y.; Moore, J. S. *Foldamers Based on Solvophobic Effects*. In *Foldamers*; Hecht, S., Huc, I., Eds.; Wiley-VCH: Weinheim, Germany, 2007; Chapter 3.

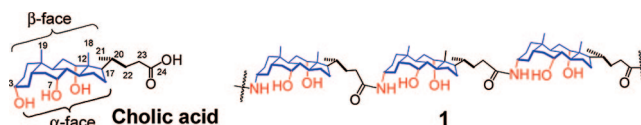
(3) For some recent examples of foldamers, see: (a) Rodríguez, J. M.; Hamilton, A. D. *Angew. Chem., Int. Ed.* **2007**, *46*, 8614–8617. (b) Dong, Z.; Yap, G. P. A.; Fox, J. M. *J. Am. Chem. Soc.* **2007**, *129*, 11850–11853. (c) Liu, S.; Zavalij, P. Y.; Lam, Y.-F.; Isaacs, L. *J. Am. Chem. Soc.* **2007**, *129*, 11232–11241. (d) Kolomiets, E.; Berl, V.; Lehn, J.-M. *Chem.–Eur. J.* **2007**, *13*, 5466–5479. (e) Baruah, P. K.; Gonnade, R.; Rajamohanan, P. R.; Hofmann, H.-J.; Sanjayan, G. J. *J. Org. Chem.* **2007**, *72*, 5077–5084. (f) Price, J. L.; Horne, W. S.; Gellman, S. H. *J. Am. Chem. Soc.* **2007**, *129*, 6376–6377. (g) Li, C.; Wang, G.-T.; Yi, H.-P.; Jiang, X.-K.; Li, Z.-T.; Wang, R.-X. *Org. Lett.* **2007**, *9*, 1797–1800. (h) Shin, S. B. Y.; Yoo, B.; Todaro, L. J.; Kirshenbaum, K. *J. Am. Chem. Soc.* **2007**, *129*, 3218–3225. (i) Yashima, E.; Maeda, K. *Macromolecules* **2008**, *41*, 3–12. (j) Meudtner, R. M.; Hecht, S. *Angew. Chem., Int. Ed.* **2008**, *47*, 4926–4930. (k) Berni, E.; Dolain, C.; Kauffmann, B.; Leger, J.-M.; Zhan, C.; Huc, I. *J. Org. Chem.* **2008**, *73*, 2687–2694. (l) Chongsirawatana, N. P.; Patch, J. A.; Czyzewski, A. M.; Dohm, M. T.; Ivankin, A.; Gidalevitz, D.; Zuckermann, R. N.; Barron, A. E. *Proc. Natl. Acad. Sci. U.S.A.* **2008**, *105*, 2794–2799. (m) Hu, H.-Y.; Xiang, J.-F.; Yang, Y.; Chen, C.-F. *Org. Lett.* **2008**, *10*, 1275–1278. (n) Han, J. J.; Shaller, A. D.; Wang, W.; Li, A. D. Q. *J. Am. Chem. Soc.* **2008**, *130*, 6974–6982. (o) Kendhale, A. M.; Gonnade, R.; Rajamohanan, P. R.; Hofmann, H.-J.; Sanjayan, G. J. *Chem. Commun.* **2008**, 2541–2543. (p) Cai, W.; Wang, G.-T.; Du, P.; Wang, R.-X.; Jiang, X.-K.; Li, Z.-T. *J. Am. Chem. Soc.* **2008**, *130*, 13450–13459. (q) Chowdhury, S.; Schantte, G.; Kraatz, H.-B. *Angew. Chem., Int. Ed.* **2008**, *47*, 7056–7059. (r) Suk, J.-m.; Jeong, K.-S. *J. Am. Chem. Soc.* **2008**, *130*, 11868–11869. (s) Merican, Z.; Johnstone, K. D.; Gunter, M. J. *Org. Biomol. Chem.* **2008**, *6*, 2534–2543.

functional groups on the side chains of α -amino acids. Notable among the 20 canonical amino acids, however, is glycine, which does not have a side chain. Even though it cannot contribute to the side-chain interactions mentioned above, glycine sometimes plays roles not duplicated by other amino acids. For example, its lack of side chains makes it easier for the peptide chains to pack together and allows certain “turn” conformations that are sterically prohibited otherwise.^{4–9}

“Strategic spacers” similar to glycine are found in synthetic foldamers as well. These are tethering groups that may not have noticeable stabilizing interactions for the folded state, but can profoundly influence the conformational properties of the foldamer. A good example of “spacer-controlled” conformation was found in the comparison of Moore’s *m*-phenylene ethynylene (*m*PE) oligomers¹⁰ and the *meta*-linked oligoresorcinols reported by Furusho, Yashima, and colleagues.¹¹ Both oligomers have aromatic phenyl units linked at the meta positions; yet dramatically different conformations result from the presence or absence of spacing units. The ethynylene spacers allow the phenyl groups in the *m*PE oligomers to stack intramolecularly, yielding single-stranded helices. Without any spacing units, the aromatic groups in the oligoresorcinols cannot stack over one another due to steric congestion. To bury the hydrophobic surface in water, two oligoresorcinol strands associate intermolecularly to form a double helix.

Ramakrishnan et al. designed polymers sensitive to alkali metal ions through a strategy that alters the length of the tethering spacers.¹² When the aromatic donor/acceptor units in the main chain were linked by tetra- or penta(ethylene glycol) units, the π - π interactions were not strong enough to overcome the conformational entropy of the tethering groups to form intramolecular charge-transfer complexes. The oligo(ethylene glycol) groups, however, contracted after complexation with alkali metal ions, triggering the intramolecular π - π stacking and charge-transfer complexation.

Iverson and co-workers investigated the effects of tethering groups on the conformation of molecules containing an aromatic donor and an acceptor,¹³ to better understand the conformation of their *aedamers* (aromatic electron donor–acceptor oligomers).¹⁴ As long as the tethering groups allowed intramolecular stacking of the aromatic groups, the folded conformation dominated, regardless of the rigidity and length of the spacers. When a para-substituted phenylene was used as the spacer, however, intramolecular stacking was geometrically prohibited and intermolecular stacking (i.e., aggregation) took place. An important lesson from this work is that tethering spacers do not have to be passive linkages. Instead, they may be used to strengthen or weaken potential noncovalent forces among the foldamer repeat units.



Our group recently reported oligocholate foldamers **1** derived from cholic acid.^{15,16} They adopt helical structures in nonpolar solvents containing a small amount of a polar solvent. In this paper, we show that insertion of 4-aminobutyroyl spacers in between the cholates profoundly influences the conformation of the oligocholates. Cooperative folding happened not only at a shorter chain length but also in more competitive solvents.

Results and Discussion

Design and Synthesis of Oligocholates with 4-Aminobutyroyl Spacers. Conformational entropy favors the unfolded, random conformation of a linear molecule over the folded, compact conformation. When an oligocholate is dissolved in a mixture of nonpolar and polar solvents, however, the conformational equilibrium is determined by the solvent composition. If the mixture contains equal amounts of polar and nonpolar solvents, both the polar (α) and nonpolar (β) faces of the cholates are well-solvated, and the unfolded conformation will dominate. If, however, the mixture is comprised largely of a nonpolar solvent (Scheme 1, blue circles) and a small amount of a polar solvent (red circles), the unfolded conformer (**U**) becomes unfavorable, as the polar faces of the cholates are exposed mostly to the nonpolar solvent. To avoid this high-energy solvophobic exposure, the oligocholate may aggregate

(4) Hamaguchi, K. *The Protein Molecule: Conformation, Stability, and Folding*; Japan Scientific Societies Press: Tokyo, Japan, 1992; p 51.

(5) Richardson, J. S.; Richardson, D. C. *Principles and Patterns in Protein Conformation. In Prediction of Protein Structure and the Principles of Protein Conformation*; Fasman, G. D., Ed.; Plenum Press: New York, 1989; Chapter 1.

(6) Rai, R.; Balaram, P. Control of Polypeptide Chain Folding and Assembly. In *Foldamers: Structure, Properties, and Applications*; Hecht, S., Huc, I., Eds.; Wiley-VCH: Weinheim, Germany, 2007; pp 147–171.

(7) (a) Ramirez-Alvarado, M.; Blanco, F. J.; Serrano, L. *Nat. Struct. Biol.* **1996**, *7*, 604–612. (b) de Alba, E.; Jimenez, M. A.; Rico, M. *J. Am. Chem. Soc.* **1997**, *119*, 175–183.

(8) (a) Maynard, A. J.; Searle, M. S. *Chem. Commun.* **1997**, 1297–1298. (b) Maynard, A. J.; Sharman, G. J.; Searle, M. S. *J. Am. Chem. Soc.* **1998**, *120*, 1996–2007. (c) Griffiths-Jones, S. R.; Sharman, G. J.; Maynard, A. J.; Searle, M. S. *J. Mol. Biol.* **1998**, *284*, 1597–1609.

(9) (a) Stanger, H. E.; Gellman, S. H. *J. Am. Chem. Soc.* **1998**, *120*, 173–180. (b) Espinosa, J. F.; Syud, J. G.; Gellman, S. H. *Protein Sci.* **2002**, *11*, 1492–1505.

(10) (a) Nelson, J. C.; Saven, J. G.; Moore, J. S.; Wolynes, P. G. *Science* **1997**, *277*, 1793–1796. (b) Prince, R. B.; Saven, J. G.; Wolynes, P. G.; Moore, J. S. *J. Am. Chem. Soc.* **1999**, *121*, 3114–3121. (c) Prince, R. B.; Okada, T.; Moore, J. S. *Angew. Chem., Int. Ed.* **1999**, *38*, 233–236. (d) Oh, K.; Jeong, K.-S.; Moore, J. S. *Nature* **2001**, *414*, 889–893. (e) Heemstra, J. M.; Moore, J. S. *Chem. Commun.* **2004**, 1480–1481. (f) Stone, M. T.; Moore, J. S. *J. Am. Chem. Soc.* **2005**, *127*, 5928–5935. (g) Goto, K.; Moore, J. S. *Org. Lett.* **2005**, *7*, 1683–1686. (h) Stone, M. T.; Heemstra, J. M.; Moore, J. S. *Acc. Chem. Res.* **2006**, *39*, 11–20. (i) Smaldone, R. A.; Moore, J. S. *J. Am. Chem. Soc.* **2007**, *129*, 5444–5450. (j) Smaldone, R. A.; Moore, J. S. *Chem.–Eur. J.* **2008**, *14*, 2650–2657.

(11) (a) Goto, H.; Katagiri, H.; Furusho, Y.; Yashima, E. *J. Am. Chem. Soc.* **2006**, *128*, 7176–7178. (b) Goto, H.; Furusho, Y.; Yashima, E. *J. Am. Chem. Soc.* **2007**, *129*, 9168–9174.

(12) (a) Ghosh, S.; Ramakrishnan, S. *Macromolecules* **2005**, *38*, 676–686. (b) Ghosh, S.; Ramakrishnan, S. *Angew. Chem., Int. Ed.* **2004**, *43*, 3264–3268.

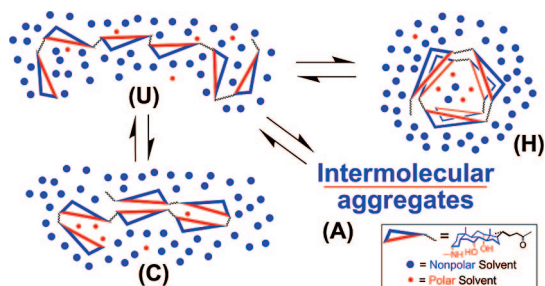
(13) Zych, A. J.; Iverson, B. L. *J. Am. Chem. Soc.* **2000**, *122*, 8898–8909.

(14) (a) Lokey, R. S.; Iverson, B. L. *Nature* **1995**, *375*, 303–305. (b) Cubberley, M. S.; Iverson, B. L. *J. Am. Chem. Soc.* **2001**, *123*, 7560–7563. (c) Gabriel, G. J.; Sorey, S.; Iverson, B. L. *J. Am. Chem. Soc.* **2005**, *127*, 2637–2640.

(15) (a) Zhao, Y.; Zhong, Z. *J. Am. Chem. Soc.* **2005**, *127*, 17894–17901. (b) Zhao, Y.; Zhong, Z. *J. Am. Chem. Soc.* **2006**, *128*, 9988–9989. (c) Zhao, Y.; Zhong, Z.; Ryu, E.-H. *J. Am. Chem. Soc.* **2007**, *129*, 218–225.

(16) For some examples of supramolecular systems constructed from cholic acid, see: (a) Davis, A. P.; Bonar-Law, R. P.; Sanders, J. K. M. In *Comprehensive Supramolecular Chemistry*; Atwood, J. L.; Davis, J. E. D., MacNicol, D. D., Vögtle, F., Eds.; Elsevier: Oxford, UK, 1996; Vol. 4, Chapter 7. (b) Li, Y.; Dias, J. R. *Chem. Rev.* **1997**, *97*, 283–304. (c) Maitra, U. *Curr. Sci.* **1996**, *71*, 617–624. (d) Zhu, X. X.; Nichifor, M. *Acc. Chem. Res.* **2002**, *35*, 539–546. (e) Smith, B. D.; Lambert, T. N. *Chem. Commun.* **2003**, 2261–2268. (f) Davis, A. P.; Joos, J.-B. *Coord. Chem. Rev.* **2003**, *240*, 143–156. (g) Virtanen, E.; Kolehmainen, E. *Eur. J. Org. Chem.* **2004**, 3385–3399. (h) Zhao, Y. *Curr. Opin. Colloid Interface Sci.* **2007**, *12*, 92–97. (i) Burrows, C. J.; Sauter, R. A. *J. Inclusion Phenom.* **1987**, *5*, 117–121. (j) Janout, V.; Lanier, M.; Regen, S. L. *J. Am. Chem. Soc.* **1996**, *118*, 1573–1574. (k) Ariga, K.; Terasaka, Y.; Sakai, D.; Tsuji, H.; Kikuchi, J.-I. *J. Am. Chem. Soc.* **2000**, *122*, 7835–7836. (l) Werner, F.; Schneider, H.-J. *J. Inclusion Phenom. Macro. Chem.* **2001**, *41*, 37–40. (m) Yoshino, N.; Satake, A.; Kobuke, Y. *Angew. Chem., Int. Ed.* **2001**, *40*, 457–459. (n) Janout, V.; Regen, S. L. *J. Am. Chem. Soc.* **2005**, *127*, 22–23.

SCHEME 1. Schematic Representations of Possible Structures of an Oligocholate in a Mixture of Polar and Nonpolar Solvents



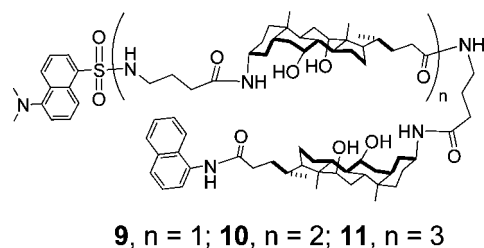
intermolecularly via hydrogen bonding of the polar groups on the cholate α -faces. An aggregate (A), however, is difficult to form if the concentration of the oligocholate is kept low. Two additional ways exist to minimize the exposure of the α -faces. The molecule may “collapse” through *intramolecular* hydrogen bonding to give a compact conformer C, or curl into a helical structure (H), in which a few polar solvent molecules are concentrated from the bulk and preferentially solvate the introverted polar groups of the oligocholates.

The parent oligocholates were found to fold into the helical conformation—a molecular model can be found in an earlier paper of ours.^{15c} Similar to other solvophobic foldamers, the folded conformers are expected to be highly dynamic.² Preferential solvation (responsible for H) was found to control both the folding of the parent oligocholates (1) and hybrid ones containing α -amino acids in the sequence. Conformer H dominated not only when the α -amino acids had non-hydrogen-bonding side chains (e.g., methionine), but also in an oligocholate containing an arginine and a glutamic acid. Although the guanidinium–carboxylate salt bridge did stabilize the folded state, intramolecular hydrogen bonding only played secondary roles.^{15c}

It is understandable that short spacers such as α -amino acids may not alter the conformation of the oligocholates greatly. After all, one α -amino acid only adds three bonds into the foldamer sequence, whereas a single cholate has at least 14 bonds from head to tail. What happens if longer, flexible spacers are introduced? The four fused rings make the cholate backbone rather rigid. Conformational freedom only exists near the carboxylic group at the end. Since rotation around C17–C20 is sterically hindered,^{16a} there are only three or four bonds capable of rotation in the entire repeat unit (see the structure of cholic acid and 1). Could these short, inflexible linkages in the oligocholates be the reason for the disfavored collapsed conformer? If so, insertion of flexible spacers in between the cholates should influence the conformation significantly.

Scheme 2 shows the synthesis of several “extended” oligocholates with 4-aminobutyryl spacers. Amino cholate 2 and the *N*-hydroxysuccinimide-activated 3 were prepared according to literature procedures^{15a,17} and reacted in anhydrous DMF to give elongated monomer 4. The Boc group was removed by HCl in methanol. Crude 5 and base-hydrolyzed 4 were allowed to couple in the presence of benzotriazol-1-yloxytris(dimethylamino)phosphonium hexafluorophosphate (BOP). The resulting dimer 6 was deprotected by acidic methanol and allowed to

react with dansyl chloride to give fluorescently labeled 7. The hydrolyzed 7 was coupled to 1-aminonaphthalene 8 to give dimer 9.



Similar chemistry was used in the preparation of trimer 10 and tetramer 11. Synthesis of 12 from 4 proceeded without any problem. However, during the deprotection of Boc, the naphthyl amide group of 12 was partially removed by HCl in methanol, even though aliphatic amides were stable under the reaction conditions. Lowering the concentration of HCl did not solve the problem, as both Boc-deprotection and naphthyl amide-methanolysis slowed down. Separation of 13 from its corresponding methyl ester (i.e., 5) by column chromatography was only partially successful due to the high polarity of these compounds. The impure 13 was used in the following amide coupling reaction (to give trimer 10). Fortunately, the methyl ester impurity of the trimer could be separated from the desired 10 by preparative TLC.

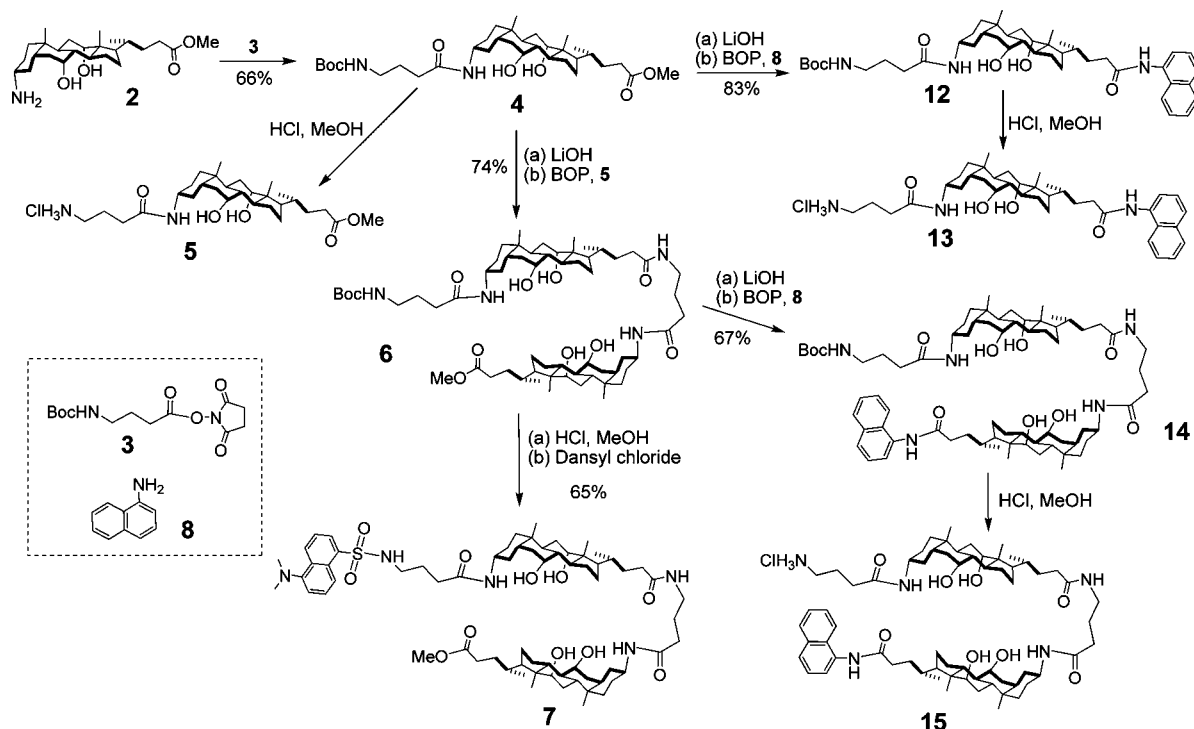
The same problem persisted in the deprotection of 14, and the separation of 15 from its corresponding methyl ester was essentially impossible. Impure 15 was used again in the amide coupling to prepare tetramer 11, which turned out to be inseparable from the tetramer methyl ester. The problem was finally solved by subjecting the mixture to basic hydrolysis. The methyl ester hydrolyzed completely in the presence of an excess of LiOH and the resulting tetramer acid could be easily separated from 11. Although the overall yield from 7 to 11 was only 27%, the combined procedures did yield a sufficient amount of the material for the characterization and the conformational study described below.

Conformational Characterization of Oligocholates with 4-Aminobutyryl Spacers. Fluorescence resonance energy transfer (FRET) is a powerful technique for conformational analysis. The energy-transfer efficiency (E) is related to the donor–acceptor (D–A) distance (r) by the following equation: $E = R_0^6 / (R_0^6 + r^6)$, in which R_0 is the Förster distance for a specific D–A pair. Because a typical R_0 (2–6 nm) is comparable to the diameters of proteins, FRET has been widely used in the conformational study of biomolecules.¹⁸

Naphthyl absorbs at 300 nm and emits around 360 nm, where dansyl has strong absorption (see Figures 1S and 5S, the UV spectra of 7 and 14, in the Supporting Information). In FRET, one ideally wants to irradiate the donor at a wavelength where the acceptor does not absorb at all (to avoid direct excitation of the acceptor), but such selectivity is rarely found. Because the largest difference in absorbance for dansyl and naphthyl occurs at 287 nm, fluorescence spectra were first collected with the compounds excited at this wavelength. Figure 1a shows the fluorescence spectra of tetramer 11 in 2:1 hexane/EA with 1–10 vol % methanol. The ternary mixture was previously identified as one of the most “folding-friendly” solvent systems for the parent oligocholates.¹⁵ Since the helical conformer (H, Scheme 1) requires the polar solvent to microphase-separate from the bulk, a lower energetic cost in the demixing is beneficial to the

(17) Guenin, E.; Monteil, M.; Bouchemal, N.; Prange, T.; Lecouvey, M. *Eur. J. Org. Chem.* **2007**, 3380–3391.

SCHEME 2. Synthesis of Oligocholates with 4-Aminobutyryl Spacers



folding. Hexane is not miscible with methanol but EA is; having hexane in the mixture thus facilitates the phase-separation of methanol.

When tetramer **11** is irradiated at 287 nm, the emission of the naphthyl donor at 360 nm is very weak whereas the acceptor emission at 480 nm is strong (Figure 1a). This behavior is

expected of FRET, in which naphthyl transfers its excited state energy to dansyl. Upon addition of methanol, the dansyl emission weakens while the naphthyl emission becomes stronger (Figure 1a, inset), indicating a decrease in the energy-transfer efficiency. Trimer **10** shows a similar behavior, although its emission intensity is about half of that of **11** to begin with

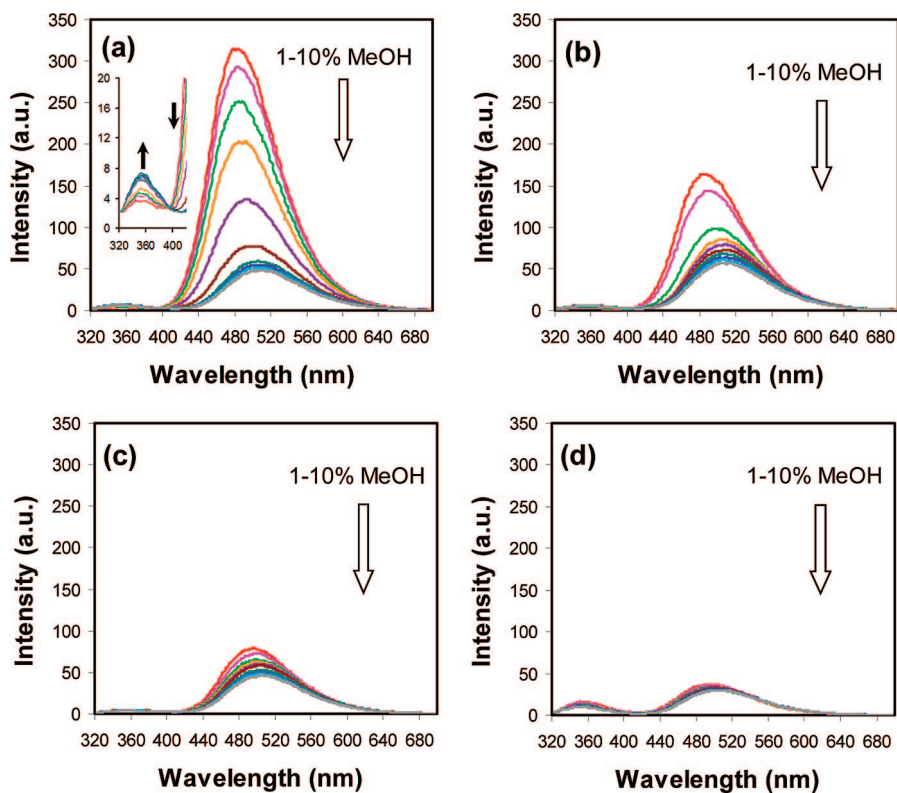


FIGURE 1. Fluorescence spectra of (a) **11**, (b) **10**, (c) **9**, and (d) the **7/14** mixture in 2:1 hexane/EA with 1–10% methanol. [oligomer] = 2.0×10^{-6} M. λ_{ex} = 287 nm.

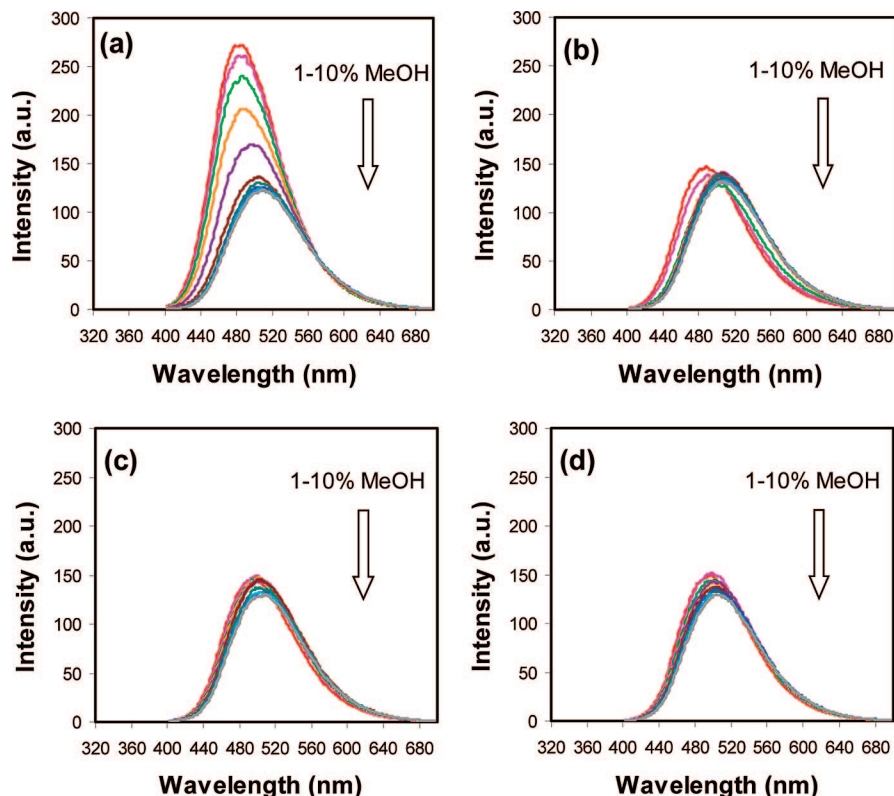


FIGURE 2. Fluorescence spectra of (a) **11**, (b) **10**, (c) **9**, and (d) the **7/14** mixture in 2:1 hexane/EA with 1–10% methanol. The excitation wavelength was 340 nm. [oligomer] = 2.0×10^{-6} M.

(Figure 1b). The folded **10** is less stable than the folded **11**. Whereas significant energy transfer (indicated by the enhanced acceptor emission) occurs in 1–5% MeOH for tetramer **11** (Figure 1a), the same is true only in 1–2% MeOH for trimer **10** (Figure 1b). Dimer **9** is probably already unfolded in 1% MeOH. The dansyl emission is less than 1/3 of that of **11** in 1% MeOH and decreases slowly and gradually as methanol is added (Figure 1c).

The fluorescence spectra of a 1:1 mixture of dimer acceptor **7** and dimer donor **14** are then recorded to probe possible intermolecular aggregation in the oligocholates. If intermolecular FRET is involved in **9–11**, energy transfer should happen in the **7/14** mixture even when the donor and the acceptor are located on different molecules. Yet, in comparison to **9–11**, the **7/14** mixture has significantly stronger naphthyl emission and weaker dansyl emission. Thus, naphthyl cannot transfer its excited state energy to dansyl in **7/14** at the same concentration (2 μ M). Since intermolecular FRET is absent in this mixture, the energy transfer observed in **9–11** most likely comes from an intramolecular process. Strictly speaking, this control experiment only excludes aggregation in dimer **9**. The longer oligomers, **10** and **11**, have more polar groups and may aggregate when the dimers do not under the same condition. This point will be addressed again later in the paper.

Parts a–d of Figure 2 show the fluorescence spectra of these compounds with $\lambda_{\text{ex}} = 340$ nm, where the naphthyl donor has no absorption. One might expect that, once FRET is switched off, the dansyl of **9–11** and the **7/14** should all behave the same. Instead, a similar weakening of dansyl emission is observed

for tetramer **11** during the methanol titration (Figure 2a). For trimer **10**, other than some spectra shift in 1–2% MeOH, the shape and intensity of the emission band remains the same throughout the titration (Figure 2b). For dimer **9** and the **7/14** dimer mixture, the dansyl emission is nearly identical and responds very little to methanol (Figure 2, parts c and d).

Thus, even without FRET, the dansyl attached to the oligocholate is still affected by the folding/unfolding process, with the longest oligocholate (**11**) experiencing the largest effect. The result is consistent with the helical conformer (more discussion in the next section). Dansyl emission is known to be solvent-sensitive.¹⁹ The helical conformer can concentrate methanol from the solvent mixture—the longer the oligocholate, the stronger this effect. Thus, local inhomogeneity of solvents should be more significant in **11** than in the shorter oligocholates. Indeed, whereas both blue shift and enhancement of emission occur in **11** in low methanol solutions (Figure 2a), only the spectra shift is observed for the shorter **10** (Figure 2b). By the time the oligomer contains two cholates, the effect disappears, as **9** and **7/14** have essentially the same emissive properties (Figure 2c,d). When the oligocholate unfolds, this inhomogeneity would also disappear and dansyl should behave the same in all the oligocholates. The spectra in high methanol solutions in parts a and d of Figure 2 confirm this point.

The idea that the locally concentrated methanol molecules enhance the dansyl emission is somewhat counterintuitive, as dansyl tends to fluoresce less strongly in more polar solvent.¹⁹ In an earlier study of ours, a solvent-sensitive chromophore (i.e., 7-nitrobenz-2-oxa-1,3-diazol-4-yl or NBD) was attached to the parent oligocholates.^{15a} Locally concentrated DMSO (the polar

(18) (a) Stryer, L. *Annu. Rev. Biochem.* **1978**, *47*, 819–846. (b) Selvin, P. R. *Methods Enzymol.* **1995**, *246*, 300–334. (c) Lakowicz, J. R. *Principles of Fluorescence Spectroscopy*, 2nd ed.; Kluwer, New York, 1999; Chapter 13.

(19) Li, Y.-H.; Chan, L.-M.; Tyer, L.; Moody, R. T.; Himel, C. M.; Hercules, D. M. *J. Am. Chem. Soc.* **1975**, *97*, 3118–3126.

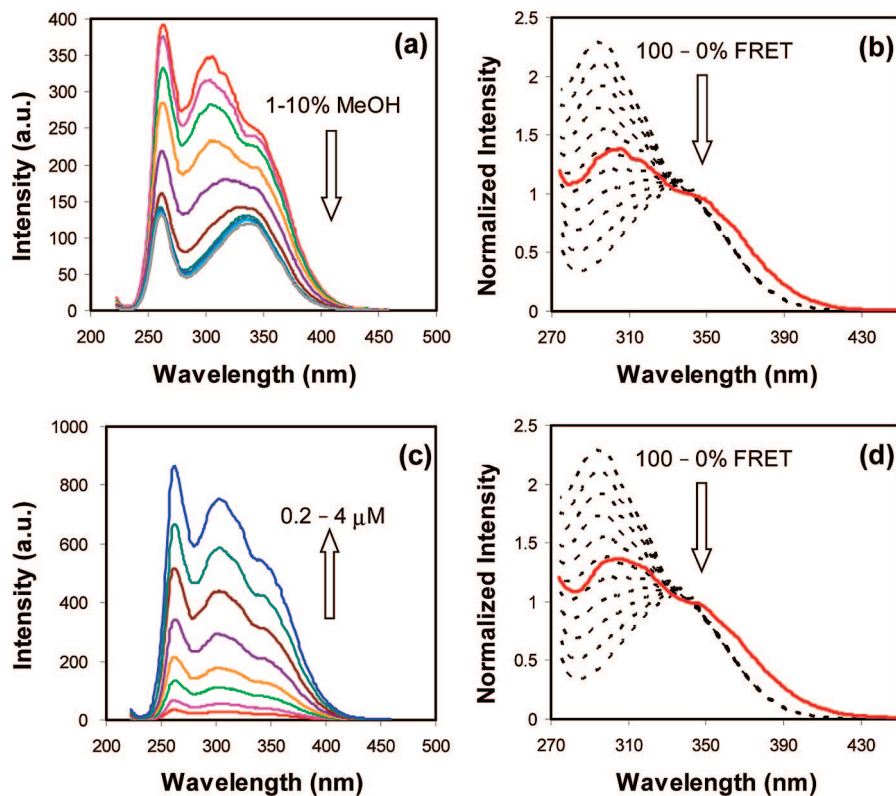


FIGURE 3. (a) Excitation spectra of **11** in 2:1 hexane/EA with 1–10% methanol. [**11**] = 2.0×10^{-6} M. (b) Normalized excitation spectrum of **11** (red) in 1% MeOH in 2:1 hexane/EA. The dotted spectra correspond to excitation spectra calculated from the absorption spectra of **7** and **14** with 100%, 90%, 80%, 70%, ..., 0% energy transfer from top to bottom. (c) Excitation spectra of different concentrations of **11** in 1% MeOH in 2:1 hexane/EA. (d) Normalized excitation spectrum of trimer **10** (red) in 1% MeOH in 2:1 hexane/EA. The acceptor emission at 500 nm was monitored.

solvent in that case) was found to affect the NBD group differently from DMSO in the bulk solvent mixture. The result was actually quite understandable because, in a generic solvent effect, the chromophore (dansyl or NBD) is completely surrounded by the polar solvent. In the folded helix, however, the polar solvent is primarily located in the hydrophilic cavity and thus the solvent shell around the chromophore is highly unsymmetrical.

It is now clear that there are two reasons for the strong dansyl emission of **11** with $\lambda_{\text{em}} = 287$ nm in low methanol solutions—the energy transfer from naphthyl and the local inhomogeneity of solvents. The excitation spectrum is useful in extracting the energy-transfer contribution. In such an experiment, the excitation wavelength is scanned while the dansyl emission at 500 nm is monitored. Without FRET, the excitation spectrum of the acceptor is similar to its absorption spectrum in shape. FRET is indicated by the appearance of the donor absorption in the excitation spectrum.¹⁸ As shown in Figure 3a, earlier during the titration, a peak is clearly visible at about 300 nm that corresponds to the absorption of naphthyl (Figure 5S, Supporting Information). This peak from the donor is visible in 1–5% MeOH for **11** and disappears after more methanol is added.

“Theoretical” excitation spectra may be obtained by adding the absorption spectrum of the donor multiplied by the energy-transfer efficiency (E) to the absorption spectrum of the acceptor.¹⁸ These are the dotted spectra in Figure 3b and may be used as references to determine E . When the excitation spectrum is normalized so that its intensity at 340 nm (the λ_{max} of the acceptor) is the same as the UV absorbance of **7** at the λ_{max} , E is found to be about 50% for **11** in 1% MeOH (Figure

3b, the red spectrum). This treatment compares the relative contribution of the donor and the acceptor to the acceptor emission, and is not affected by the local inhomogeneity of solvents. Whether the excited state energy of the acceptor comes from the direct excitation of the acceptor or the energy transfer from the donor, the emission is subjected to the same influence. Interestingly, the same treatment shows the energy-transfer efficiency for trimer **10** also to be 50% in 1% MeOH (Figure 3d).

Note that some spectra shift is observed between the normalized excitation spectrum and the calculated, dotted ones. The shift is expected because the excitation spectrum is recorded in 1% MeOH in 2:1 hexane/EA whereas the absorption spectra are recorded in 10% MeOH/EA. Since the R_0 of the naphthyl–dansyl pair is 2.2 nm,²⁰ 50% energy-transfer efficiency gives an average D–A distance of 2.2 nm in 1% MeOH. The energy-transfer efficiency is about 10% in 6% MeOH (Figure 6S, Supporting Information), which translates to a D–A distance of 3.2 nm. By the time 10% methanol is added to the solution, the normalized excitation spectrum of **11** is indeed identical with the absorption spectrum of **7** (Figure 7S, Supporting Information), indicating the absence of FRET.

As discussed earlier, although the lack of FRET in the **7/14** mixture rules out aggregation of the dimers, aggregation of the longer oligocholates is still a concern. Figure 3c shows the excitation spectra of **11** in 1% MeOH over a concentration range

(20) (a) Stryer, L.; Haugland, R. P. *Proc. Natl. Acad. Sci. U.S.A.* **1967**, *58*, 719–726. (b) Haas, E.; Wilchek, M.; Katchalski-Katzir, E.; Steinberg, I. Z. *Proc. Natl. Acad. Sci. U.S.A.* **1975**, *72*, 1807–1811.

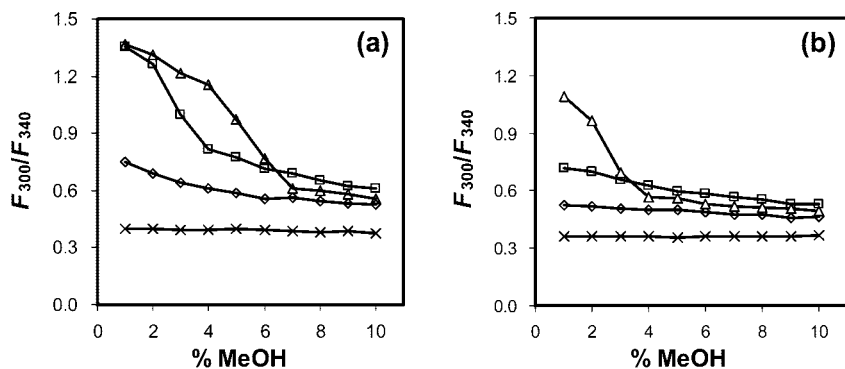


FIGURE 4. F_{300}/F_{340} of **11** (Δ), **10** (\square), **9** (\diamond), and the **7/14** mixture (\times) as a function of methanol percentage in (a) 2:1 hexane/EA and in (b) EA. F_{300} and F_{340} represent the emission intensity of dansyl at 500 nm in the excitation spectrum at 300 and 340 nm ($=\lambda_{\text{ex}}$), respectively. [oligomer] = 2.0×10^{-6} M. The data points are connected to guide the eye.

of 0.2–4 μM . With the longest oligomer in the most nonpolar solvents, this condition represents the most “aggregation-prone”. Yet, the shape of the excitation spectrum is independent of concentration. In fact, the normalized excitation spectra of **11** overlap almost exactly with one another during the concentration change (Figure 8S, Supporting Information), demonstrating that the energy-transfer efficiency ($E \approx 50\%$) is the same during the 20-fold dilution. Furthermore, when the emission intensity of the dansyl is plotted against concentration, the linear relationship is obtained whether λ_{ex} is 287 or 340 nm (Figure 9S, Supporting Information). These results strongly suggest the absence of aggregation in **11**. Although trimer **10** is less likely to aggregate, similar experiments are performed (Figures 10S–12S, Supporting Information), showing no signs of aggregation as well.

Because λ_{max} for the donor and acceptor is 300 and 340 nm, respectively, the ratio of dansyl emissions at 300 and 340 nm in the excitation spectrum (i.e., F_{300}/F_{340}) is a good indicator for the energy-transfer efficiency. A higher F_{300}/F_{340} indicates a larger contribution of the naphthyl donor to the dansyl emission, and corresponds to a shorter D–A distance. Figure 4a compares the F_{300}/F_{340} ratio of these extended oligocholates in the MeOH/hexane EA = 2:1. Figure 4b shows the same relationship in a binary solvent mixture, MeOH/EA. As mentioned earlier, hexane facilitates the phase separation of methanol; its removal from the solvent mixture thus should destabilize the folded state.

The solvent-titration curve (i.e., F_{300}/F_{340} vs % MeOH) for the **7/14** mixture (\times) is completely flat and lies below all the other curves (Figure 4a). This is simply because there is no FRET at all throughout the titration. The curve for dimer **9** (\diamond) shows a slow, gradual decline, but is sigmoidal for both the trimer **10** (\square) and the tetramer **11** (Δ). Sigmoidal titration curves are characteristic of cooperative conformational changes.²¹ They were only observed for the parent oligocholates with at least five cholate groups.^{15a} It is remarkable that even the trimer and tetramer show cooperative behavior for the extended oligocholates.

When hexane is removed from the solvent mixture, the F_{300}/F_{340} ratio is essentially the same for **7/14** (compare parts a and b of Figure 4, \times), but is lower on the left side (the folded region) in every single case for **9** (\diamond), **10** (\square), and **11** (Δ). Thus, as expected, a smaller population of the folded state is found in EA than in hexane/EA with the same percentage of methanol. Notably, the tetramer still has a sigmoidal titration curve (Figure

4b, Δ). Apparently, only the longest oligocholate is able to fold in MeOH/EA. Overall, the extended oligocholates can fold far better than the parent oligocholates without spacers. For example, even the hexamer and heptamer of the parent oligocholates could not fold in the MeOH/EA mixture.¹⁵

Collapsed versus Helical Conformation for the Extended Oligocholates. The collapsed conformer (**C**, Scheme 1) is stabilized by intramolecular hydrogen bonds. Therefore, the more hydrogen bonds the folded conformer can form, the more stable it should be. Face-to-face interaction is the dominant motif in the solid state structure of cholic acid derivatives.²² If a similar motif is involved in conformer **C**, one would expect an odd/even effect. In other words, dimer **9** can fold in the middle and satisfy the hydrogen bonding sites of both cholates. Tetramer **11** can fold either in the middle (allowing two cholates to interact with another two) or at the 1,3 position (so that a terminal cholate can hydrogen bond with its immediate neighbor). Trimer **10**, however, would be in an awkward situation. No matter how it folds, one-third of the hydrogen bonds cannot be satisfied.

Folding of the extended oligocholates clearly does not follow the odd/even trend. Parts a and b of Figure 4 both suggest that the stability of the folded state increases with the chain length. Both the chain length effect and the sigmoidal titration curves support **H** as the folded state. In a two-state conformational change such as helix-coil transition,²¹ the folded and unfolded states exist simultaneously during the transition and interconvert as the environmental conditions are varied (eq 1). The two-state model works particularly well for solvophobic foldamers with relatively rigid repeat units.^{10b,15a}



Indeed, the titration curves for the trimer (\square) and the tetramer (Δ) fit well to the two-state model (Figure 5a). The details of the data analysis are described in the Experimental Section. A characteristic feature of a two-state transition is a linear dependence of folding free energy on the concentration of the “denaturant” (methanol in this case), which is confirmed for both **11** and **10** (Figure 5b).

Cooperative conformational change is frequently observed in proteins. It is remarkable that the extended oligocholates can display cooperative folding with as few as three repeat units.

(22) For two reviews, see: (a) Miyata, M.; Sada, K. In *Comprehensive Supramolecular Chemistry*; Atwood, J. L., Davis, J. E. D., MacNicol, D. D., Vögtle, F., Eds.; Elsevier: Oxford, UK, 1996; Vol. 6, Chapter 6. (b) Miyata, M.; Sada, K.; Yoswathananont, N. In *Encyclopedia of Supramolecular Chemistry*; Atwood, J. L., Steed, J. W., Eds.; Marcel Dekker: New York, 2004; p 441.

(21) Chan, H. S.; Bromberg, S.; Dill, K. A. *Philos. Trans. R. Soc. London B* **1995**, *348*, 61–70.

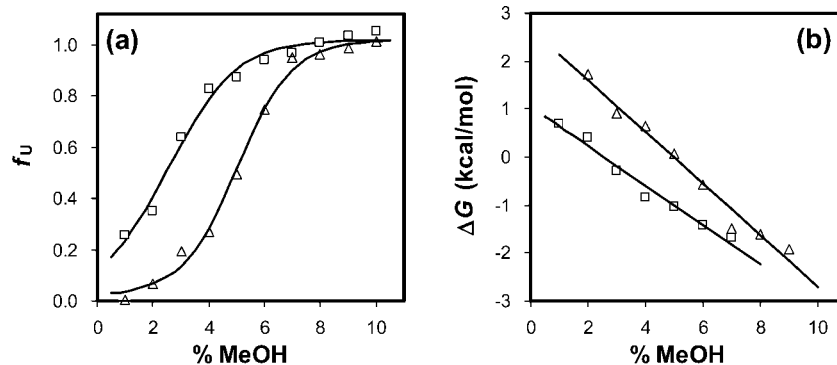


FIGURE 5. (a) Fraction of the unfolded conformer in **11** (Δ) and **10** (\square) as a function of the volume percentage of MeOH in 2:1 hexane/EA. The theoretical curves are nonlinear least-squares fitting to a two-state transition model. (b) Unfolding free energies for **11** (Δ) and **10** (\square) as a function of solvent composition and linear fits of the data (see the Experimental Section for details).

One of the most accepted models for protein cooperativity is the “hydrophobic core collapse”.²¹ When multiple side chains of a peptide chain cluster together in water, *all* the hydrophobic groups in this core benefit by avoiding unfavorable hydration. (Cooperativity, thus, does not require a highly organized, discrete, folded state.) In water, the solvophobic (i.e., hydrophobic) effect demands a *direct* contact of solvophobic surfaces. The solvophobic effect in the oligocholates uses the phase-separated polar solvents to *mediate* the hydrogen-bonding interactions of the polar groups. Since this effect is driven by avoiding the contact between the polar faces of the cholates and the nonpolar solvents, referring to it as solvophobic is a reasonable choice. Despite the difference between the two effects, the physical basis for cooperativity seems amazingly similar. Each additional unit in the oligocholate makes the foldamer more capable of concentrating the polar solvent into the folded helix. The result is better solvation of the introverted polar groups for *all* the cholate groups in a largely nonpolar solvent mixture.

Parts b and d of Figure 3 indicate that the energy-transfer efficiency is 50% for both **10** and **11** in 1% MeOH. The average D–A distance (ca. 2.2 nm) is thus the same. (This apparently is a coincidence, as the energy-transfer efficiencies for the two are very different in 1% MeOH/EA, as shown by Figure 4b.) The two-state data fitting allows the determination of the percentage of the folded or unfolded conformer at any given solvent composition. As shown by Figure 5a, ~2% of the tetramer and 20% of the trimer are unfolded in 1% MeOH. Given the same average distance, these unfolded fractions indicate that the D–A distance *for the folded state* is smaller in the trimer than in the tetramer.²⁴ This result, of course, is more consistent with the trimeric periodicity observed in the parent oligocholates.^{15a} What is more interesting is that a similar trimeric periodicity seems to be maintained even in the unfolded states. The titration curves in parts a and b of Figure 4 both show the same order of trimer > tetramer > dimer on the right side (i.e., the unfolded region). Thus, the average D–A distance for the unfolded structures is also smaller in the trimer than either the dimer or the tetramer. This trend cannot be explained

by a typical random conformer (in which the D–A distance should increase with the chain length). It appears that somehow the unfolded state “remembers” the trimeric periodicity of the folded conformation. Preference for the trimer was reported separately by Sanders and co-workers in cyclic oligocholate esters.²³ In this latter case, the hydroxyl groups at the C7 and C12 of the cholic acid were either eliminated or protected and no amphiphilic driving force existed to fold the oligocholate esters. Preference for the trimeric periodicity apparently resulted from the curvature of the cholate backbone. It is possible that the unfolded state, at least when it is not too far from the folding/unfolding equilibrium, may have a similar preference.

An attempt was made to study the conformation of the extended oligocholates by ¹H NMR spectroscopy. A mixture of deuterated methanol and carbon tetrachloride was used instead of the ternary mixture. At NMR concentrations (e.g., submillimolar), however, **11** aggregated extensively in 2–4% MeOH/CCl₄ and gave broad NMR peaks. A further increase of methanol in the mixture did sharpen the signals, but the NMR spectrum was independent of solvent composition above 5% MeOH, presumably because the oligocholate was already unfolded.

Conclusions

Insertion of flexible 4-aminobutyroyl spacers into the oligocholates indeed has a large impact on the conformation. The helical folding mechanism seems to be maintained but the folded state becomes significantly more stable. Even the trimer (**10**) and the tetramer (**11**) of the extended oligocholates display cooperative folding. What could be the possible reason for the improved foldability? Previously, our group prepared amphiphilic molecular baskets by attaching cholate groups to a cone-shaped scaffold such as calix[4]arene or hexasubstituted benzene.²⁵ These molecules adopt reversed micelle-like conformation similar to the folded oligocholate helix: both have inwardly facing polar groups solvated by the polar solvent phase-separated from the bulk. Flexible spacers between the cholates and the scaffold were found to facilitate the phase-separation of DMSO-*d*₆ from CCl₄ into the molecular baskets.^{25c} Most likely, flexible linkers allow the cholates to turn their polar faces inward without introducing much strain. This effect, of course, is beneficial whether the cholates are organized on a covalent

(23) Brady, P. A.; Bonar-Law, R. P.; Rowan, S. J.; Suckling, C. J.; Sanders, J. K. M. *Chem. Commun.* **1996**, 319–320.

(24) Energy-transfer efficiency and unfolded fraction themselves do not allow the calculation of the D–A distance for the folded state because the D–A distance for the unfolded state is unknown. Because the energy transfer mainly comes from the folded state, a smaller population of the folded trimer and the same average energy-transfer efficiency for both oligocholates indicate a more efficient energy transfer for the folded trimer.

(25) (a) Ryu, E.-H.; Zhao, Y. *Org. Lett.* **2004**, *6*, 3187–3189. (b) Zhao, Y.; Ryu, E.-H. *J. Org. Chem.* **2005**, *70*, 7585–7591. (c) Ryu, E.-H.; Yan, J.; Zhong, Z.; Zhao, Y. *J. Org. Chem.* **2006**, *71*, 7205–7213.

scaffold as in the molecular baskets or in a head-to-tail fashion as in the oligocholates. Overall, the role of the 4-aminobutyroyl spacers in the oligocholates is surprisingly similar to that of glycine in the “turn” conformations.^{4–9}

With the rapid development of foldamers, chemists should pay attention not only to functional monomers that provide the primary driving force to the folding but also to spacers that can profoundly influence the foldability. In the oligocholates, introduction of 4-aminobutyroyl spacers does not alter the folding mechanism. As shown by the *m*PE foldamers¹⁰ and oligoresorcinols,¹¹ however, different spacers may make similar backbones adopt completely different conformations.

Experimental Section

General Procedure I (Deprotection of Boc). Acetyl chloride (3–5 mmol) was slowly added to MeOH (10–20 mL).²⁶ The resulting HCl solution was added to a solution of the Boc-protected compound (1 mmol) in MeOH (2–5 mL). After 24–48 h at room temperature, MeOH was removed by rotary evaporation. The residue was filtered through a plug of silica gel, using CH₂Cl₂/MeOH mixtures as the eluent, and used in the next step (i.e., amide coupling) directly.

General Procedure II (Hydrolysis of Methyl Ester). The methyl ester (1 mmol) was dissolved in methanol (5 mL) and was stirred with 2 M LiOH (5 mL, 10 mmol) at room temperature. Reaction was monitored by TLC and was complete in 5–24 h. Upon completion, most methanol was removed by rotary evaporation. The residue was quenched with 2 N HCl until pH 3–4. The acid product was either extracted with EA or collected by suction filtration, and was generally used in the following amide coupling reaction without further purification.

Compound 4. Compounds **2** (1.512 g, 3.59 mmol)^{15a} and **3** (1.87 g, 3.74 mmol)¹⁷ were dissolved in anhydrous DMF (25 mL). Diisopropylethylamine (DIPEA, 0.7 mL, 4.0 mmol) was added. After 2 h at room temperature, the mixture was diluted with water (40 mL) then extracted with EtOAc (60 mL). The organic layer was washed with 0.5 M H₂SO₄ until pH ~3, dried over MgSO₄, concentrated by rotary evaporation, and chromatographed over silica gel, using CH₂Cl₂/CHCl₃ = 1/1 with 6% MeOH as eluents to give a white foam (2.495 g, 66% yield). ¹H NMR (400 MHz, DMSO) δ 7.69 (d, *J* = 8.0 Hz, 1 H), 6.74 (t, *J* = 5.6 Hz, 1 H), 4.10–4.04 (m, 2H), 3.75 (br, 1H), 3.58 (br, 1H), 3.53 (s, 3H), 3.28 (br, 1H), 2.85–2.79 (m, 2H), 2.33–2.07 (m, 4H), 1.99–1.89 (m, 3H), 1.81–0.81 (series of m, 32H), 0.80 (s, 3H), 0.55 (s, 3H); ¹³C NMR (100 MHz, CDCl₃) δ 174.9, 172.3, 56.6, 79.1, 73.0, 73.0, 72.9, 68.35, 68.30, 68.27, 68.22, 68.15, 55.8, 51.7, 51.6, 49.5, 47.1, 46.4, 42.0, 41.9, 40.3, 39.5, 35.4, 35.0, 34.8, 34.0, 32.5, 31.2, 31.1, 28.6, 27.7, 26.4, 24.8, 23.3, 22.8, 17.4, 14.3, 12.6; MALDI-TOFMS (*m/z*) [M + H]⁺ calcd for C₃₄H₅₉N₂O₇ 607.8, found 608.4; [M + Na]⁺ calcd for C₃₄H₅₈N₂O₇Na 629.8, found 630.3.

Compound 6. Hydrolyzed compound **4** (104 mg, 0.175 mmol, prepared according to General Procedure II), compound **5** (100 mg, 0.184 mmol, prepared according to General Procedure I), 1-hydroxybenzotriazole hydrate (HOBt, 25 mg, 0.185 mmol), and BOP (122 mg, 0.276 mmol) were dissolved in anhydrous DMF (5 mL). DIPEA (212 mg, 0.936 mmol) was added. The reaction mixture was stirred at 50 °C under N₂ for 66 h. DMF was removed by rotary evaporation and the residue was purified by column chromatography over silica gel with CH₂Cl₂/MeOH = 20/1 to 6/1 as the eluents to give a white foam (141 mg, 74% yield). ¹H NMR (400 MHz, DMSO) δ 7.69 (m, 3 H), 6.74 (t, *J* = 5.6 Hz, 1 H), 4.08–4.03 (m, 4H), 3.75 (br, 2H), 3.57 (br, 2H), 3.53 (s, 3H), 3.28 (br, 1H), 2.95–2.88 (m, 2 H), 2.85–2.79 (m, 2 H), 2.31–0.81 (series of m, 70H), 0.80 (s, 6H), 0.55 (s, 3H), 0.54 (s, 3H); ¹³C

NMR (100 MHz, CDCl₃/CD₃OD = 4:1) δ 175.52, 175.46, 173.1, 173.0, 157.0, 73.0, 68.2, 54.6, 54.0, 51.7, 49.8, 47.3, 47.1, 47.0, 46.5, 42.8, 42.1, 41.9, 39.8, 39.6, 38.8, 36.3, 35.8, 35.6, 34.9, 34.7, 33.9, 33.4, 32.1, 31.3, 31.2, 28.5, 28.3, 27.7, 27.5, 26.6, 26.4, 25.8, 23.4, 22.8, 18.9, 17.32, 17.26, 12.6; MALDI-TOFMS (*m/z*) [M + H – Boc]⁺ calcd for C₅₇H₉₇N₄O₉ 982.4, found 982.0; [M + Na]⁺ calcd for C₆₂H₁₀₄N₄O₁₁Na 1104.5, found 1104.3.

Compound 7. Deprotected compound **6** (266 mg, 0.271 mmol, prepared according to General Procedure I) and DIPEA (149 mg, 1.15 mmol) were dissolved in anhydrous CH₂Cl₂ (5 mL). Dansyl chloride (92 mg, 0.341 mmol) was added. The mixture was stirred under N₂ at room temperature for 24 h. Solvent was removed by rotary evaporation and the residue was purified by column chromatography over silica gel with CH₂Cl₂/CHCl₃ = 1/1 with 8% MeOH to give a yellow foam (215 mg, 65% yield). ¹H NMR (400 MHz, CDCl₃/CD₃OD = 4:1) δ 8.45 (d, *J* = 8.8 Hz, 1H), 8.23 (d, *J* = 6.8 Hz, 1H), 8.11 (d, *J* = 6.4 Hz, 1H), 7.88 (d, *J* = 8.4 Hz, 1H), 7.53–7.43 (m, 2H), 7.13 (d, *J* = 7.6 Hz, 1H), 3.75 (br, 2H), 3.59 (s, 3H), 3.56 (s, 3H), 3.46 (br, 2H), 3.11 (t, *J* = 6.8 Hz, 2H), 2.81 (s, 6H), 2.78 (t, *J* = 7.2 Hz, 2 H), 2.36–0.78 (series of m, 60H), 0.83 (s, 6H), 0.61 (s, 6H); ¹³C NMR (100 MHz, CDCl₃/CD₃OD = 4:1) δ 175.54, 175.45, 175.34, 173.0, 172.9, 172.7, 172.6, 151.8, 135.0, 130.2, 129.8, 129.6, 129.2, 128.2, 123.2, 119.0, 115.3, 109.0, 77.7, 77.6, 77.4, 77.0, 72.9, 68.1, 51.6, 49.6, 48.9, 48.4, 46.3, 45.4, 39.3, 38.7, 36.2, 35.8, 35.5, 35.4, 34.5, 33.7, 33.4, 33.1, 31.8, 31.1, 31.0, 28.1, 27.2, 26.4, 25.6, 23.2, 22.5, 17.2, 17.1, 12.42, 12.39; MALDI-TOFMS (*m/z*) [M + H]⁺ calcd for C₆₉H₁₀₈N₅O₁₁S 1215.7, found 1215.0; [M + Na]⁺ calcd for C₆₉H₁₀₇N₅NaO₁₁S 1237.7, found 1236.0.

Compound 9. Hydrolyzed compound **7** (91 mg, 0.075 mmol, prepared according to General Procedure II), 1-aminonaphthalene **8** (22 mg, 0.15 mmol), HOBt (15 mg, 0.11 mmol), and BOP (73 mg, 0.16 mmol) were dissolved in anhydrous DMF (1.5 mL). DIPEA (80 mg, 0.62 mmol) was added. The reaction mixture was stirred at 55 °C under N₂ for 43 h. The mixture was poured into acid water (3 mL of 2 N HCl in 40 mL of water). The precipitate was collected by suction filtration and purified by column chromatography over silica gel with CH₂Cl₂/MeOH = 20/1 to 6/1 as the eluents to give a light brown glass (57 mg, 57% yield). ¹H NMR (400 MHz, CDCl₃/CD₃OD = 4:1) δ 8.46 (d, *J* = 8.4 Hz, 1H), 8.23 (d, *J* = 8.4 Hz, 1H), 8.11 (d, *J* = 7.2 Hz, 1H), 7.88 (d, *J* = 8.4 Hz, 1H), 7.79 (d, *J* = 8.4 Hz, 1H), 7.66 (d, *J* = 8.4 Hz, 1H), 7.59 (d, *J* = 7.2 Hz, 1H), 7.53–7.28 (m, 4H), 7.20–7.11 (m, 2H), 3.94 (br, 1H), 3.90 (br, 1H), 3.76 (br, 5H), 3.45 (br, 2H), 3.15–3.07 (m, 2H), 2.82 (s, 6H), 2.77 (t, *J* = 6.4 Hz, 2 H), 2.58–2.48 (m, 1H), 2.44–2.34 (m, 1H), 2.23–0.73 (series of m, 63H), 0.66 (s, 3H), 0.62 (s, 3H); ¹³C NMR (100 MHz, CDCl₃/CD₃OD = 4:1) δ 175.6, 175.5, 174.6, 173.1, 172.8, 151.8, 134.9, 134.2, 130.3, 128.5, 128.2, 125.5, 123.3, 121.9, 119.0, 115.5, 115.3, 77.6, 75.8, 73.1, 73.0, 68.2, 51.7, 49.6, 46.8, 46.4, 45.4, 41.8, 41.7, 38.9, 35.7, 34.8, 33.5, 32.0, 29.7, 28.1, 25.6, 23.2, 22.6, 17.3, 17.2, 12.5, 12.4; MALDI-TOFMS (*m/z*) [M + H]⁺ calcd for C₇₈H₁₁₃N₆O₁₀S 1326.8, found 1326.6.

Compound 12. Hydrolyzed compound **4** (100 mg, 0.169 mmol, prepared according to General Procedure II), 1-aminonaphthalene **8** (49 mg, 0.34 mmol), HOBt (24 mg, 0.18 mmol), and BOP (149 mg, 0.347 mmol) were dissolved in anhydrous DMF (2 mL). DIPEA (110 mg, 0.85 mmol) was added. The reaction mixture was stirred at 50 °C under N₂ for 68 h. DMF was removed by rotary evaporation and the residue was purified by column chromatography over silica gel with CH₂Cl₂/MeOH = 20/1 to 12/1 as the eluents to give a white foam (100 mg, 83% yield). ¹H NMR (400 MHz, DMSO) δ 9.82 (s, 1H), 8.02–7.98 (m, 1H), 7.92–7.88 (m, 1H), 7.74–7.88 (m, 3H), 7.53–7.42 (m, 3H), 7.35 (t, *J* = 7.6 Hz, 1 H), 6.75 (t, *J* = 5.2 Hz, 1 H), 4.11–4.00 (m, 2H), 3.80 (br, 1H), 3.58 (br, 1H), 3.08 (br, 1H), 2.82 (q, *J* = 6.4 Hz, 2 H), 2.42–0.83 (series of m, 38H), 0.81 (s, 3H), 0.59 (s, 3H); ¹³C NMR (100 MHz, CDCl₃/CD₃OD = 4:1) δ 174.7, 157.0, 134.3, 132.8, 128.5, 126.8, 126.3, 125.7, 122.7, 122.1, 117.0, 111.3, 79.4, 73.2, 68.4, 54.9, 47.0, 46.6,

(26) Nudelman, A.; Bechor, Y.; Falb, E.; Fischer, B.; Wexler, B. A.; Nudelman, A. *Synth. Commun.* **1998**, *28*, 471–474.

43.0, 41.9, 39.8, 39.5, 36.4, 36.0, 35.7, 34.9, 34.6, 33.9, 33.6, 32.1, 28.5, 28.2, 27.8, 27.4, 26.6, 26.3, 23.4, 22.7, 18.9, 17.4, 12.7, 12.6; MALDI-TOFMS (m/z) [$M + H - \text{Boc}$] $^+$ calcd for $\text{C}_{38}\text{H}_{56}\text{N}_3\text{O}_4$ 618.9, found 619.7; [$M + \text{Na}$] $^+$ calcd for $\text{C}_{43}\text{H}_{63}\text{N}_3\text{NaO}_6$ 741.0, found 741.3.

Compound 14. Hydrolyzed compound **6** (190 mg, 0.178 mmol, prepared according to General Procedure II), 1-aminonaphthalene **8** (55 mg, 0.38 mmol), HOBt (24 mg, 0.18 mmol), and BOP (124 mg, 0.280 mmol) were dissolved in anhydrous DMF (1.5 mL). DIPEA (130 mg, 1.0 mmol) was added. The reaction mixture was stirred at 55 °C under N_2 for 71 h. The mixture was poured into acid water (3 mL of 2 N HCl in 40 mL of water). The precipitate was collected by suction filtration and purified by column chromatography over silica gel with EA/MeOH = 8/1 to 6/1 as the eluents to give an off-white powder (143 mg, 67% yield). ^1H NMR (400 MHz, DMSO) δ 9.82 (s, 1H), 8.02–7.98 (m, 1H), 7.91–7.87 (m, 1H), 7.73–7.67 (m, 4H), 7.60 (d, $J = 7.6$ Hz, 1H), 7.52–7.47 (m, 1H), 7.44 (t, $J = 8.0$ Hz, 1H), 6.74 (t, $J = 5.2$ Hz, 1H), 4.11–3.99 (m, 4H), 3.80 (br, 1H), 3.75 (br, 1H), 3.58 (br, 1H), 3.08 (br, 1H), 2.95–2.88 (m, 2H), 2.85–2.78 (m, 2H), 2.40–0.75 (series of m, 78H), 0.59 (s, 3H), 0.54 (s, 3H); ^{13}C NMR (100 MHz, $\text{CDCl}_3/\text{CD}_3\text{OD} = 4:1$) δ 175.6, 174.7, 173.2, 157.1, 134.4, 132.8, 128.6, 128.5, 126.5, 126.3, 126.1, 125.6, 122.7, 122.1, 79.4, 73.2, 73.1, 68.3, 49.8, 47.0, 46.5, 42.0, 41.9, 39.9, 39.8, 39.5, 39.0, 36.4, 36.0, 35.8, 34.9, 34.6, 33.9, 33.7, 33.5, 32.1, 28.4, 28.2, 27.7, 27.4, 26.6, 26.3, 25.7, 23.3, 22.7, 17.4, 17.3, 12.5; MALDI-TOFMS (m/z) [$M + H - \text{Boc}$] $^+$ calcd for $\text{C}_{66}\text{H}_{102}\text{N}_5\text{O}_8$ 1093.5, found 1092.8; [$M + \text{Na}$] $^+$ calcd for $\text{C}_{71}\text{H}_{109}\text{N}_5\text{NaO}_{10}$ 1215.6, found 1215.2.

Compound 10. Hydrolyzed compound **7** (36 mg, 0.030 mmol, prepared according to General Procedure II), compound **13** (21 mg, 0.032 mmol, prepared according to General Procedure I), HOBt (7 mg, 0.05 mmol), and BOP (40 mg, 0.09 mmol) were dissolved in anhydrous DMF (1.5 mL). DIPEA (60 mg, 0.46 mmol) was added. The reaction mixture was stirred at 55 °C under N_2 for 24 h. The mixture was poured into acid water (1.5 mL of 2 N HCl in 40 mL of water). The precipitate was collected by suction filtration and purified by preparative TLC with $\text{CHCl}_3/\text{MeOH}/\text{AcOH} = 160/20/3$ as the solvents to give a light brown glass (29 mg, 54% yield). ^1H NMR (400 MHz, $\text{CDCl}_3/\text{CD}_3\text{OD} = 4:1$) δ 8.46 (d, $J = 8.4$ Hz, 1H), 8.23 (d, $J = 8.8$ Hz, 1H), 8.11 (d, $J = 7.2$ Hz, 1H), 7.88 (d, $J = 7.2$ Hz, 1H), 7.79 (d, $J = 8.4$ Hz, 1H), 7.66 (d, $J = 8.0$ Hz, 1H), 7.60 (d, $J = 7.6$ Hz, 1H), 7.53–7.29 (m, 4H), 7.20–7.11 (m, 2H), 3.94 (br, 1H), 3.89 (br, 2H), 3.75 (br, 3H), 3.46 (br, 3H), 3.16–3.06 (m, 4H), 2.82 (s, 6H), 2.79 (t, $J = 6.4$ Hz, 2H), 2.58–2.48 (m, 1H), 2.45–2.34 (m, 1H), 2.22–0.75 (series of m, 100H), 0.66 (s, 3H), 0.61 (s, 6H); ^{13}C NMR (100 MHz, $\text{CDCl}_3/\text{CD}_3\text{OD} = 4:1$) δ 175.6, 175.5, 174.5, 173.1, 173.0, 172.8, 172.7, 151.8, 135.0, 134.2, 32.7, 129.9, 128.2, 126.0, 123.3, 122.5, 121.9, 119.0, 115.3, 77.6, 73.1, 13.0, 68.2, 49.7, 49.6, 46.8, 46.5, 46.4, 45.4, 41.8, 41.7, 39.4, 38.7, 35.7, 34.5, 33.5, 33.2, 31.9, 29.7, 28.1, 26.4, 25.6, 23.2, 22.6, 17.3, 17.2, 12.5, 12.4; MALDI-TOFMS (m/z) [$M + \text{H}$] $^+$ calcd for $\text{C}_{106}\text{H}_{159}\text{N}_8\text{O}_{14}\text{S}$ 1801.5, found 1800.3.

Compound 11. Hydrolyzed compound **7** (43 mg, 0.036 mmol, prepared according to General Procedure II), compound **15** (42 mg, 0.037 mmol, prepared according to General Procedure I), HOBt (5 mg, 0.04 mmol), and BOP (36 mg, 0.081 mmol) were dissolved in anhydrous DMF (1 mL). DIPEA (40 mg, 0.31 mmol) was added. The reaction mixture was stirred at 55 °C under N_2 for 15 h. The mixture was poured into acid water (1.5 mL of 2 N HCl in 40 mL of water). The precipitate was collected by suction filtration and purified by column chromatography over silica gel with EA/MeOH = 4/1 to 3/1 as the eluents to a crude product that contained both compound **11** and the corresponding methyl ester. The mixture was hydrolyzed with LiOH (0.4 mL, 2M) in MeOH (6 mL). Product **11** was separated from the corresponding carboxyl impurity by column chromatography over silica gel with $\text{CH}_2\text{Cl}_2/\text{CHCl}_3 = 1/1$ with 15–25% MeOH as the eluents (22 mg, 27% yield). ^1H NMR

(400 MHz, $\text{CDCl}_3/\text{CD}_3\text{OD} = 4:1$) δ 8.45 (d, $J = 8.4$ Hz, 1H), 8.23 (d, $J = 8.8$ Hz, 1H), 8.11 (d, $J = 7.6$ Hz, 1H), 7.87 (d, $J = 7.6$ Hz, 1H), 7.79 (d, $J = 8.8$ Hz, 1H), 7.65 (d, $J = 7.6$ Hz, 1H), 7.61 (d, $J = 7.2$ Hz, 1H), 7.53–7.28 (m, 4H), 7.17–7.11 (m, 2H), 3.74 (br, 4H), 3.60 (br, 4H), 3.46 (br, 4H), 3.15–3.06 (m, 6H), 2.81 (s, 6H), 2.78 (t, $J = 6.4$ Hz, 2H), 2.58–2.47 (m, 1H), 2.43–2.33 (m, 1H), 2.22–0.72 (series of m, 134H), 0.65 (s, 3H), 0.61 (s, 9H); ^{13}C NMR (100 MHz, $\text{CDCl}_3/\text{CD}_3\text{OD} = 4:1$) δ 175.8, 175.7, 175.6, 175.2, 173.1, 173.0, 172.8, 151.8, 135.0, 134.2, 129.2, 128.5, 128.4, 128.2, 125.5, 123.3, 122.6, 122.0, 119.0, 115.3, 77.6, 73.1, 73.0, 68.3, 49.7, 49.6, 49.5, 46.7, 46.43, 46.38, 45.4, 41.9, 41.7, 39.4, 38.7, 35.9, 34.5, 33.7, 33.1, 31.9, 29.7, 28.1, 25.7, 25.4, 23.2, 22.6, 17.3, 17.2, 12.5, 12.4; MALDI-TOFMS (m/z) [$M + \text{H}_3\text{O} + \text{H}$] $^{2+}$ calcd for $\text{C}_{134}\text{H}_{207}\text{N}_{10}\text{NaO}_{19}\text{S}$ 1158.6, found 1158.5; [$M + \text{Na}$] $^+$ calcd for $\text{C}_{134}\text{H}_{204}\text{N}_{10}\text{NaO}_{18}\text{S}$ 2298.2, found 2297.8.

Fluorescence Experiments. Stock solutions (2.0×10^{-4} M) of **9**, **10**, **11**, and an equimolar mixture of **7** and **14** in 10% MeOH/EA were prepared. An aliquot (20.0 μL) of the stock solution was diluted by 2.00 mL of hexane/EA ($v/v = 12/1$) with 1 vol % methanol in a quartz cuvette. Nine aliquots of MeOH (20.0 μL each) were added to the sample. After each addition, the sample was vortexed for 0.5 min before the fluorescence spectrum was recorded.

Data Analysis. According to the two-state model, at any given concentration of the denaturant (i.e., MeOH), only the folded and unfolded conformations are present and their fractions are represented by f_{F} and f_{U} . The fraction of the unfolded conformation can be calculated by:

$$f_{\text{U}} = (R_{\text{F}} - R)/(R_{\text{F}} - R_{\text{U}}) \quad (2)$$

in which R is the observed F_{300}/F_{340} ratio for the foldamer, R_{F} is the F_{300}/F_{340} ratio in the fully folded conformer, and R_{U} is the F_{300}/F_{340} ratio in the fully unfolded conformer. The equilibrium constant (K_{eq}) and the free energy (ΔG) for the folding reaction can be calculated by using the following

$$\Delta G = -RT \ln K_{\text{eq}} = -RT \ln(f_{\text{F}}/f_{\text{U}}) = -RT \ln\{f_{\text{U}}/(1 - f_{\text{U}})\} \quad (3)$$

In the two-state model, the free energies are linearly related to the concentration of denaturant (i.e., MeOH):

$$\Delta G = \Delta G_0 - m[\text{MeOH}] \quad (4)$$

From eqs 2, 3, and 4, we can obtain eq 5, which describes the relationship between f_{U} and MeOH percentage, and eq 6, which describes the relationship between R and MeOH percentage:

$$f_{\text{U}} = 1/\{1 + 1/\exp[-(\Delta G_0 - m[\text{MeOH}])/RT]\} \quad (5)$$

$$R = R_{\text{F}} - f_{\text{U}}(R_{\text{F}} - R_{\text{U}}) = R_{\text{F}} - (R_{\text{F}} - R_{\text{U}})/\{1 + 1/\exp[-(\Delta G_0 - m[\text{MeOH}])/RT]\} \quad (6)$$

A nonlinear least-squares fitting of the experimental data to eq 6 afforded R_{F} and R_{U} . These numbers were plugged into eq 2 to give f_{U} (Figure 5a) and into eq 3 to give ΔG (Figure 5b) at different solvent composition.

Acknowledgment. The author acknowledges the NSF (CHE-0748616) and the Roy J. Carver Charitable Trust for support of this research.

Supporting Information Available: General experimental methods, additional figures, and NMR data. This material is available free of charge via the Internet at <http://pubs.acs.org>.

JO802201B